

Automatic active acoustic target detection in turbulent aquatic environments

Shaun Fraser,^{1*} Vladimir Nikora,¹ Benjamin J. Williamson,² Beth E. Scott²

¹School of Engineering, University of Aberdeen, Aberdeen, UK

²School of Biological Sciences, University of Aberdeen, Aberdeen, UK

Abstract

There is no established approach for dealing with the active acoustic detection of biological targets in highly dynamic aquatic environments where intense physical interference means that standard techniques are unsuitable. This is a particular problem in ecologically important environments with emerging industrial significance such as marine energy extraction sites. We developed an automatic processing method which allows effective target detection with high sensitivity throughout variable acoustic conditions. The method is based on scale-dependent adaptive filtering of data and morphological analysis of short-scale backscatter contributions for the exclusion of intense turbulent features and isolation of biological targets. Echosounder platform deployments around marine energy infrastructure in a tidal channel provide test data which demonstrate the effectiveness of the proposed approach. Target validation and assessment is carried out by the analysis of multifrequency characteristics and direct inspection. The results deliver effective, quantitative, and repeatable assessment of ecological interactions and target distributions with clear implications for environmental assessment in high energy sites and promising applications in other contexts.

Target detection in turbulent environments is a challenge in many applications of hydroacoustic analysis. Beyond the operational difficulties of collecting data in demanding conditions, there is no established approach for the processing, analysis, and interpretation of hydroacoustic data at high turbulence levels. Turbulence in marine environments can lead to high magnitudes of acoustic backscatter due to the suspension of sediments (Thorne and Hanes 2002), entrainment of air (Plueddemann et al. 1996; Trevorrow 1998), and steep gradients in water density (Lavery et al. 2003; Moum et al. 2003). This can lead to effective operational turbulence limits for acoustic analysis and data gaps in time or space for particularly dynamic conditions and sites.

Maintaining consistent functionality of hydroacoustic instrumentation is a particular problem for the monitoring requirements of marine energy devices. A particular challenge is investigating the unknown effects of tidal stream generator technologies on ecological interactions in high energy sites (Scott et al. 2014; Benjamins et al. 2015). Effective environmental impact assessment requires continuous high resolution monitoring and automated data processing around

marine energy installations (Polagye et al. 2014). These installations are naturally built in the most energetic environments available for maximum energy yield, although the strong tidal flows lead to extreme turbulence at a range of scales (Lu et al. 2000; Thomson et al. 2012). The use of standard biological sampling techniques such as nets and trawls is impractical in such conditions, and the use of cameras for optical monitoring is impossible most of the time due to the low effective range. Thus, despite the difficulties, hydroacoustic analysis is the only practical means of continuous ecological monitoring around marine energy installations.

Tidal channels are some of the most dynamic and challenging environments for hydroacoustic work, and have led to the rise of many recent innovative approaches in data collection and analysis using moving vessels (Jacques 2014; Melvin and Cochrane 2015), moored boats (Viehman et al. 2014), and bottom-mounted platforms (Jacques 2014; Wiesbron 2015; Williamson et al. 2015). Although ship based echosounder surveys are the general approach in fisheries research for most applications, the use of stationary platforms can have distinct advantages (Joslin et al. 2014; Williamson et al. 2015). A major advantage is the ability to monitor a specific point in space over longer time scales than could be achieved with the operational limitations of a vessel in the high tidal flows. The use of a platform mounted on the seabed also removes problems associated with vessel

*Correspondence: s.fraser@abdn.ac.uk

This is an open access article under the terms of the Creative Commons Attribution License, which permits use, distribution and reproduction in any medium, provided the original work is properly cited.

noise and behavioral impacts from the ship during the analysis and interpretation of hydroacoustic data.

Many types of acoustic instruments are available for platform deployments including: passive acoustic hydrophones, acoustic cameras, single beam echosounders, multibeam echosounders, and multifrequency split beam scientific echosounders. Acoustic cameras offer advantages in resolution while multibeam echosounders provide greater coverage. However, the multifrequency scientific echosounder is the focus here since it is the only technology which can currently provide calibrated measurements of backscatter over the entire depth of a typical tidal channel over multiple useful frequencies. These characteristics are essential to classify species and to understand the full vertical distribution and behavior of targets in these sites.

The use of hydroacoustics to monitor biological targets generally relies on established calibration, processing, and analysis techniques. For the delineation of fish schools in scientific echosounder data, this generally involves using standard image processing techniques (Barange 1994) and expert scrutiny to identify and classify backscattering bodies against background noise and interference from other biological sources and physical effects (Horne 2000; Reid et al. 2000). This process is further informed using multifrequency information and prior knowledge of the backscattering characteristics and behavior of the targets of interest to separate fish from plankton (Kang et al. 2002; Sato et al. 2015) or to identify specific fish species when possible (Kloser et al. 2002; Logerwell and Wilson 2004; Korneliussen et al. 2009).

These established approaches rely on applying a minimum backscatter strength threshold on available data from a particular frequency or some combination of frequencies to delineate pixels of interest (Simmonds and MacLennan 2005). This simple approach is widely used in the initial processing of echosounder data as it is functional in the majority of fisheries applications where the background conditions are acoustically stable. However, in highly dynamic and turbulent aquatic environments, the background acoustic characteristics can be extremely variable (Fig. 1) leading to the failure of standard processing approaches for target detection. The fundamental difficulty in reliable target detection is dealing with turbulent sources of backscatter which can be of comparable backscatter strength (Melvin and Cochrane 2015) as the biological targets of interest and overlapping in time and space.

Recent work to identify targets in tidal channels has used a variety of approaches. Viehman and Zydlewski (2014) relied on manual processing of acoustic camera data employing a frame-by-frame analysis for fish identification, characterization, and behavioral interpretation. Similarly in the echosounder work of Melvin and Cochrane (2015), the identification of fish and isolation of turbulence effects were based on the authors' experience. In the mobile surveys of Jacques (2014) and Jacques and Horne (2014), the standard school

detection algorithm used in Echoview (Myriax Software, v.5.4.91) and based on the work of Barange (1994) was employed to identify turbulent features as apparent "schools" that intersect a line three meters from the echosounder transducers mounted on the ship. Other groups have opted to exclude the near surface environment altogether, for example, in the single beam work of Staines et al. (2015) and Viehman et al. (2014) the upper 10 m of the water column was excluded due to interference from entrained air. This highlights another advantage of collecting data from the near-seabed region, as measurements are taken below the intense backscatter observed in the near-surface turbulent layer and so are free from this short-range interference. However, even with stationary bottom-mounted platform surveys, backscatter from the turbulent surface layer can dominate the water column. In analysis undertaken by Wiesebron (2015) a constant backscatter threshold was applied and analysis constrained to a bottom layer 25 m thick in an area of 55 m total water depth. Similarly, in the recent work of Viehman and Zydlewski (2015), the echosounder beam was oriented horizontally and restricted to a 40 m range giving a maximum height of 10 m from the seabed at the far limit in 25–30 m deep water. Viehman and Zydlewski (2015) used a single target detection algorithm (Ona and Barange 1999) available in Echoview (Myriax Software, v.6.1) which cannot identify individuals within schools or aggregations.

Processing approaches which seriously limit the depth range or temporal continuity of analysis cannot possibly give a full understanding of the behavior of fish and other targets of interest at highly dynamic sites. Target detection approaches which tolerate false contributions from physical backscatter sources or which use inflexible algorithms that exclude substantial true targets, will inevitably lead to inaccurate environmental assessments and biased results. Similarly, manual processing approaches can never be practical for the long datasets available from platform deployments which are necessary to investigate behavior over the full range of tidal scales with seasonal influences, nor can manual processing ever provide a systematic tool for comparison between different research groups studying different sites. The challenge here was to extract the maximum possible reliable information from hydroacoustic data in these difficult environments regardless of depth and conditions. We are primarily concerned with detecting aggregations of resident fish. Although marine mammals and diving birds are also detectable in the data used here, fish targets are frequent enough to design and assess an optimized detection method. Similarly, the detection of persisting ecological layers linked to seasonal or daily trends is not the concern of this paper. Instead, the main goal of this paper relates to the detection of discrete aggregations of fish capable of independent movement in the strong flows, which we call targets.

To achieve this overall goal, we present a flexible methodology capable of target detection over the challenging

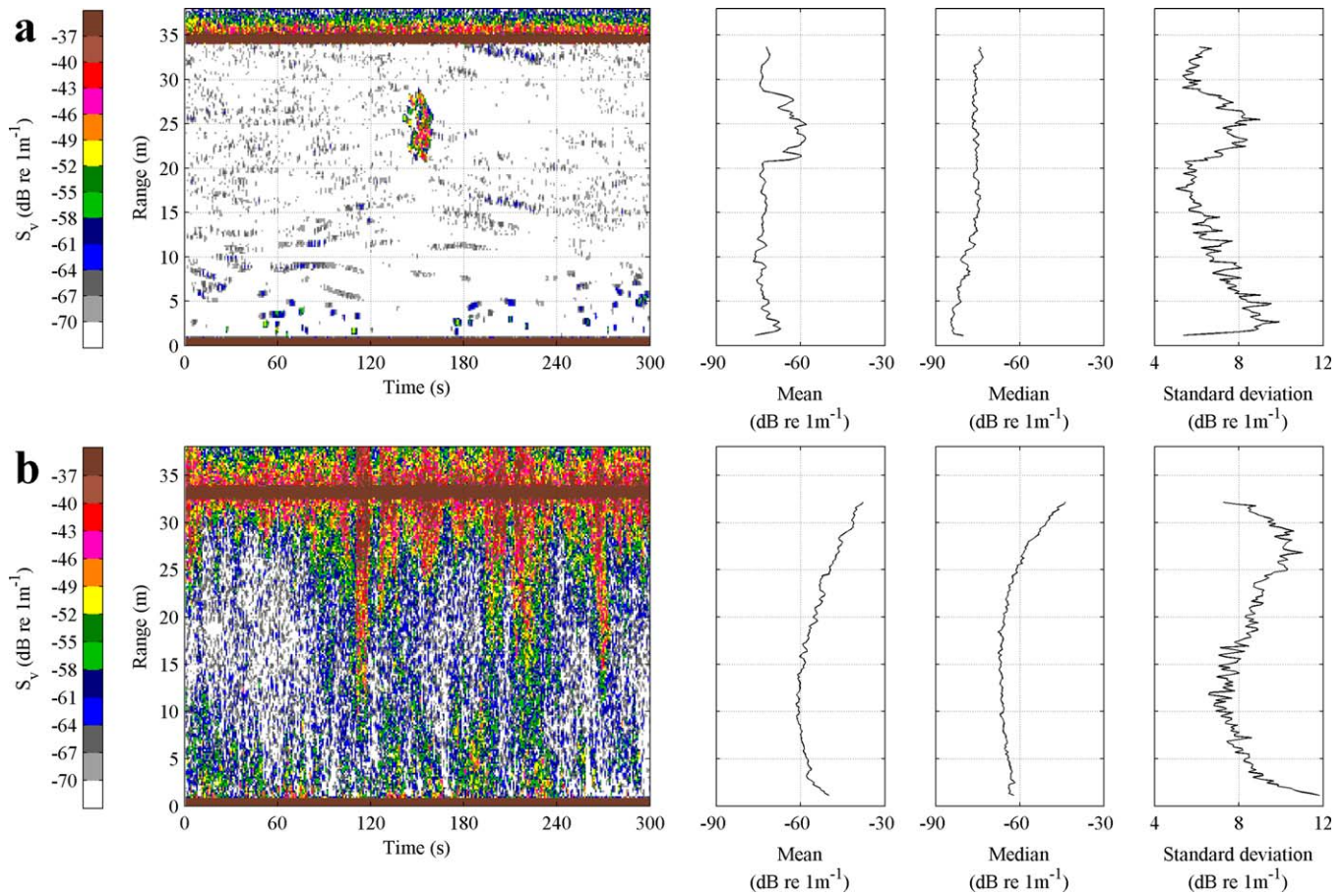


Fig. 1. Comparison of volume backscattering strength (S_v) data and statistics recorded by an upward facing stationary platform at the Fall of Warness, UK, in June 2013. **(a)** Calm weather and low flow conditions where there are limited physical sources of S_v and detection of biological targets is relatively straightforward. An aggregation of fish is clearly visible at 25 m range persisting for approximately 30 s. Mean, median, and standard deviation are calculated through time across each row of S_v data and show relatively stable behavior with depth except in the presence of targets. **(b)** Turbulent conditions during high winds and high tidal flow where elevated S_v and unstable statistics are present across the entire water column and particularly near the sea surface making effective detection of biological targets challenging. Prior processing approaches would lead to the nondetection of the clear target in **(a)** in some cases, and the inclusion of the much of the turbulent backscatter in **(b)** as valid targets in other cases.

conditions encountered in marine renewable energy sites. This paper describes the development of an automatic, repeatable, and sensitive approach for target detection based on scale-dependent adaptive filtering and the morphological exclusion of turbulent backscatter. This provides an effective and timely method applicable to emerging requirements and other hydroacoustic applications in turbulent aquatic environments.

Materials and procedures

The data presented in this article and the initial motivation for the development of the proposed method come from echosounder platform deployments in a tidal channel (Williamson et al. 2014). To establish an effective processing approach for the detection of targets, various standard and novel techniques for target detection were explored. The strengths and weaknesses of different techniques generally

depended on the physical conditions and varied significantly in complexity, sensitivity, and flexibility. Although some of these techniques are briefly discussed, we mainly focus on the description of a proposed method which uses the simplest and most effective approach. This proposed method is outlined in Fig. 2 which serves to guide the method described step-by-step in the following sections.

Data collection

Deployments of the FLOWBEC-4D platform (FLOW, Water column and Benthic Ecology 4-D) were performed at the European Marine Energy Centre (EMEC) test sites, UK (Williamson et al. 2014). These deployments gathered multifrequency echosounder data with synchronized multibeam echosounder measurements (Williamson et al. 2015) and were further supported by hydrodynamic model data for the sites (Waggitt et al. 2016). This paper uses datasets collected

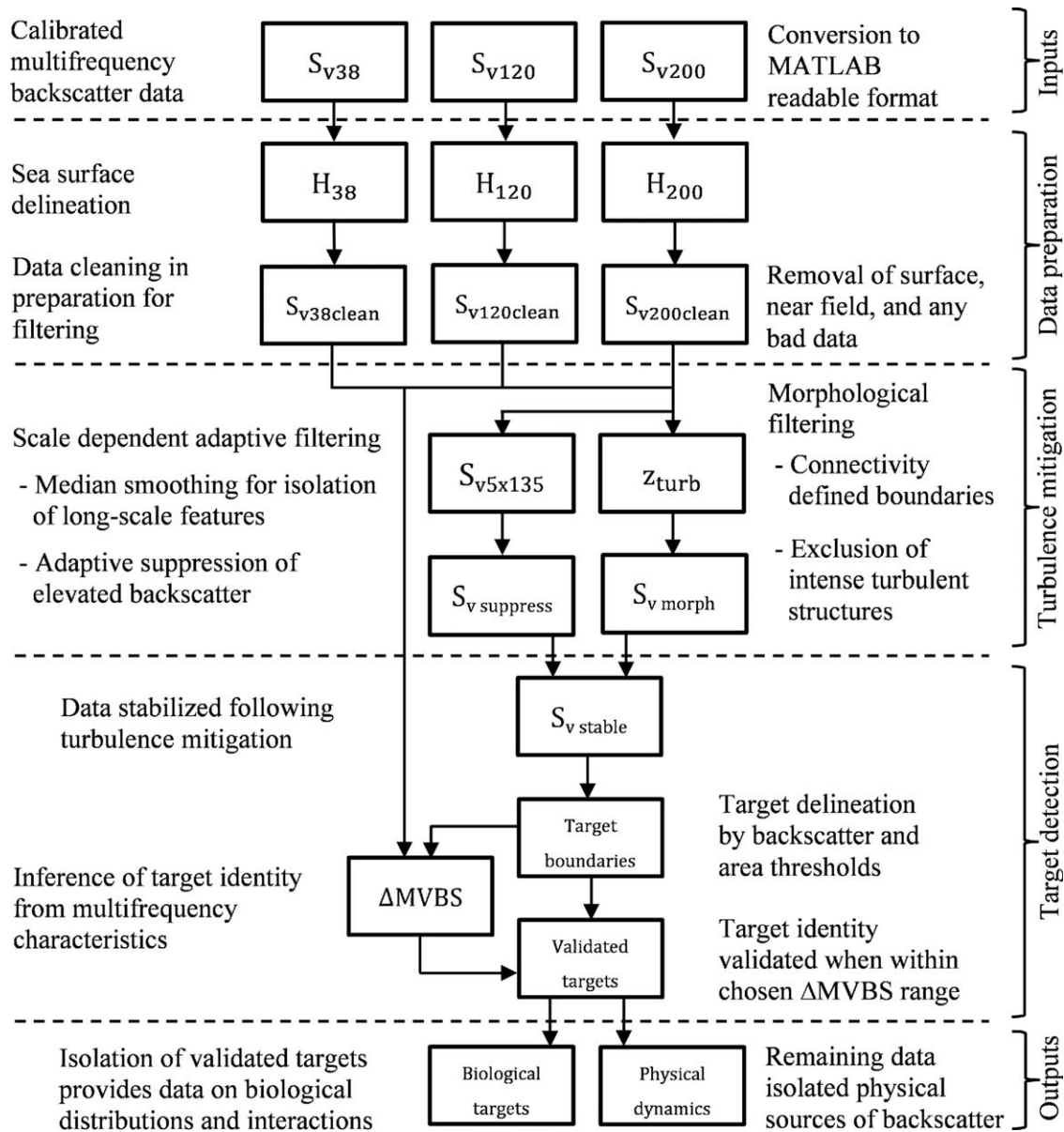


Fig. 2. Conceptual outline of proposed target detection methodology. This shows an overview from the input of raw multifrequency data through the processing steps and validation process to provide effective target detection. All parameters and processes are defined fully in subsequent sections.

in a tidal channel during two platform deployments at the full scale tidal test site at the Fall of Warness, UK ($59^{\circ}11'N$, $2^{\circ}47'$ to $2^{\circ}50'W$), at approximately 35 m depth during summer 2013. The first deployment was positioned 20 m downstream (during the flood phase) from an Atlantis AK-1000 turbine tripod base and piling and recorded data from June 3rd to June 15th. The second deployment was positioned nearby in the same site for recording control data out of the wake of any turbine structures from June 18th to July 5th.

The conditions at the Fall of Warness were the most challenging encountered during platform deployments and data

analysis so far. This tidal channel is characterized by exceptionally strong tidal flows exceeding 4 m s^{-1} . The complex coastline and bathymetry lead to powerful shear features in the wake of headlands and islands, with large eddies, upwelling boils, and overturning turbulent motions across the site. Periodic tidal dynamics combine with variable meteorological conditions to generate complex wave-current interactions and intense surface dynamics especially during windy periods.

The platform uses a multifrequency split beam Simrad EK60 scientific echosounder with 38, 120, and 200 kHz transducers. These are orientated directly upwards with

overlapping 7° conical beams. All EK60 transducers ping simultaneously at 1 Hz using a 1024 μs pulse length and were calibrated using a 38.1 mm tungsten carbide sphere following standard procedures (Foote et al. 1987).

Preprocessing

Initial data inspection and quality control were performed using Echoview (Myriax Software, v5.3). Thereafter, all processing and analysis were done in the MATLAB (MathWorks, R2013a) programming environment using custom scripts. Initial data conversion into a MATLAB readable format used the readEKRaw MATLAB toolkit (by Rick Towler, NOAA Alaska Fisheries Science Center). This facilitated full flexibility in data handling beyond the tools available in Echoview.

Calibrated raw backscatter values are expressed in the logarithmic measure of volume backscatter strength (S_v in dB re 1 m^{-1}) for each of the three frequencies (S_{v38} , S_{v120} , and S_{v200}). Backscatter data are plotted in echograms generally over the range -70 dB to -37 dB which is a useful viewing range for the detection of targets and visualization of turbulence. The apparent range resolution of each ping is dependent on the pulse length and the resulting echosounder vertical sampling thickness, so for the data here is approximately 0.19 m. Near field effects (Simmonds and MacLennan 2005) are removed using a frequency dependent constant range. This sets an effective minimum range for target detection for each frequency which was approximately 6.3 m for 38 kHz, 2.1 m for 120 kHz, and 1.2 m for 200 kHz. The 200-kHz dataset is the focus of many of the subsequent processing steps due to its superior performance at low range.

Surface detection

The first stage of data processing was the identification of the strong returns from the sea surface and exclusion of pixels at and beyond the sea surface range (H). This is achieved using a line-picking algorithm based on a minimum threshold for surface backscatter. This is similar to bottom-detecting approaches and data exclusion in downward facing echosounders in conventional mobile ship based surveys. However, while the strong backscatter from the seabed boundary is generally easy to identify, in the case of sea surface detection precise distinction is often difficult. This is because the energetic conditions can lead to strong wave action and a disturbed surface obscured by a strongly reflecting turbulent layer of aerated water near the sea surface (Crawford and Farmer 1987; Deane et al. 2013). The threshold to delineate the surface effectively over the changing conditions and with minimal exclusion of data is selected using the Otsu segregation technique (Otsu 1975). This unsupervised technique defines the optimal threshold to separate the probability distributions of classes of pixels in an image by minimizing the combined intra-class variance, and as shown in Fig. 3 is found to be -32 dB during a 5-d section of 200 kHz data between 1.2 m and 37.9 m range. A

line picking algorithm defines H for each ping by identifying the lowest ranged pixel which is greater than the threshold -32 dB and is contiguous with the pixel identified as having the highest S_v value (and so assumed to be part of the sea surface reflection). The resulting surface range for each frequency (H_{38} , H_{120} , and H_{200}) is tested by inspection throughout the dataset and by power spectrum analysis of the H time series which shows consistent close agreement between frequencies. Although the beam width at the surface (approximately 4 m) acts as low-pass filter for H and the vertical resolution of H is limited by the echosounder sampling thickness, clear tide and wave behavior is apparent as shown in Fig. 3. Power spectral density estimates are calculated using the average of 50% overlapping 30 min H sections using a Hamming window over one tidal cycle.

The preprocessed data uses the H time series with a 0.5 m subtraction for safety to exclude any other spurious backscatter contributions from the surface. This gives $S_{v \text{ clean}}$ data for each frequency which is the basis for all quantitative backscatter measurements and the next steps of data processing. In the absence of turbulence and strong variations in the background acoustic conditions the data would now be ready for standard school detection algorithms. However, the dominance of turbulent backscatter would lead to overwhelming numbers of false targets reflecting the effects of turbulent structures over multiple spatial and temporal scales. For reliable target detection, turbulence mitigation measures are essential and described in the following proposed processing steps.

Scale-dependent adaptive filtering

Backscatter in highly energetic sites is dominated by intense physical processes which vary over length and time scales leading to extremely unstable conditions in which to identify biological targets. In particular, tidal conditions and meteorological effects which vary over the course of hours lead to broad variations in backscatter statistics through time and over the water column depth. Applying sensitive (i.e., lower) thresholds to the data to detect biological targets, which would work effectively in calm conditions, would lead to numerous false targets in turbulent conditions. Conversely, applying less sensitive thresholds to the data to avoid false targets in turbulent conditions will prevent the detection of many genuine targets. The crude approach would be to simply remove “bad” data which is deemed too turbulent or noisy to process; however, in the application here this would involve excluding the majority of available data and biasing results.

To investigate the dominant time scales present in backscatter data we can use wavelet analysis. Wavelet analysis is particularly useful for the data here since the relatively short-scale intermittent presence of targets combined with broad physical features in the data leads to highly statistically non-stationary backscatter variations. The potential of

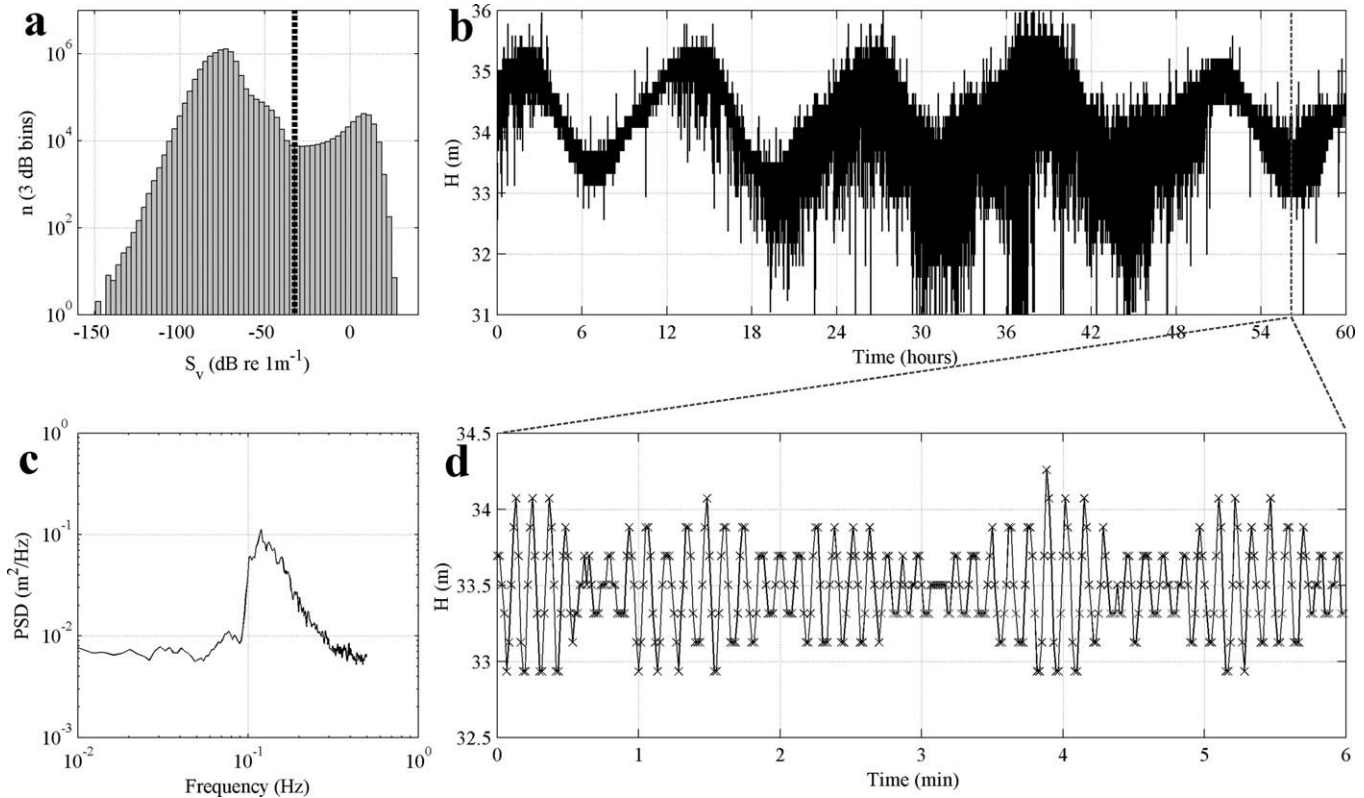


Fig. 3. Sea surface delineation and validation by optimal surface threshold line-picking algorithm. **(a)** The number (n) of S_v samples in 3 dB bins during a flood-ebb cycle using 200 kHz data with near field removed. The thick dashed line indicates the threshold used to separate backscatter dominated by sea surface reflections (on the right of the line) from the remaining water column. **(b)** The resulting time series for H showing the variable short-scale surface wave propagation superimposed on top of the dominant long-scale tidal height variation. **(c)** The resulting power spectrum for H which shows a clear dominant surface wave frequency of order 0.1 Hz. **(d)** A short section of H highlighted by the grey dashed line in **(b)** showing clear surface wave propagation over the echosounder beam.

wavelet analysis for ecological time series has been recognized widely and has been used to look for patterns in time and frequency domains in a variety of contexts (Cazelles et al. 2008). However, there is limited work that utilizes echosounder data (e.g., Bertrand et al. 2008; Jacques 2014). The wavelet power spectrum used here for the data interpretation follows the approach of Torrence and Compo (1998) using a Ricker (often referred to as the “Mexican hat”) mother wavelet (Torrence and Compo 1998).

As the largest fish schools recorded persist for approximately 1 min in the data then on longer time scales (hours) the wavelet power spectra are dominated by backscatter from the physical dynamics. However, in Fig. 4 we look specifically at relatively short time scales (minutes) to investigate the scales of fish schools and moderate near-surface turbulence. Wavelet power spectra from a depth averaged section of $S_{v200\text{clean}}$ shows how the non-stationary contributions from biological targets can be conceptually separated from physical backscatter by considering scale. Depth specific and 2D wavelet transforms are also possible. However, the capability of a target detection method based on wavelet results is limited by the physical and biological

backscatter contributions which overlap in mean and the reduced power of targets with relatively low mean S_v . Nonetheless the practical mitigation of long-scale turbulent backscatter contributions is possible and scale sensitive filtering is essential.

We use a moving window operation which acts as a selective 2D high pass filter to isolate target-scale structures. To facilitate processing flexibility and reliability, an adaptive approach is used to suppress backscatter through time and depth during elevated backscatter. This is equivalent to adapting the target detection thresholds themselves (Nero and Magnuson 1989) when necessary to avoid false detections. This is achieved by the selective subtraction of the data from a scale-sensitive smoothed “background” version of the data produced by the filter. Sophisticated wavelet denoising methods (e.g., Donoho 1995) or Eigenvector filtering (e.g., Baussant et al. 1993) could be used to construct the smoothed data; however, for simplicity and flexibility a moving window median operation is the preferred method here. As the mean is computed for the linear expression of backscatter (normally considered in logarithmic units) then mean values are highly sensitive to strong backscattering

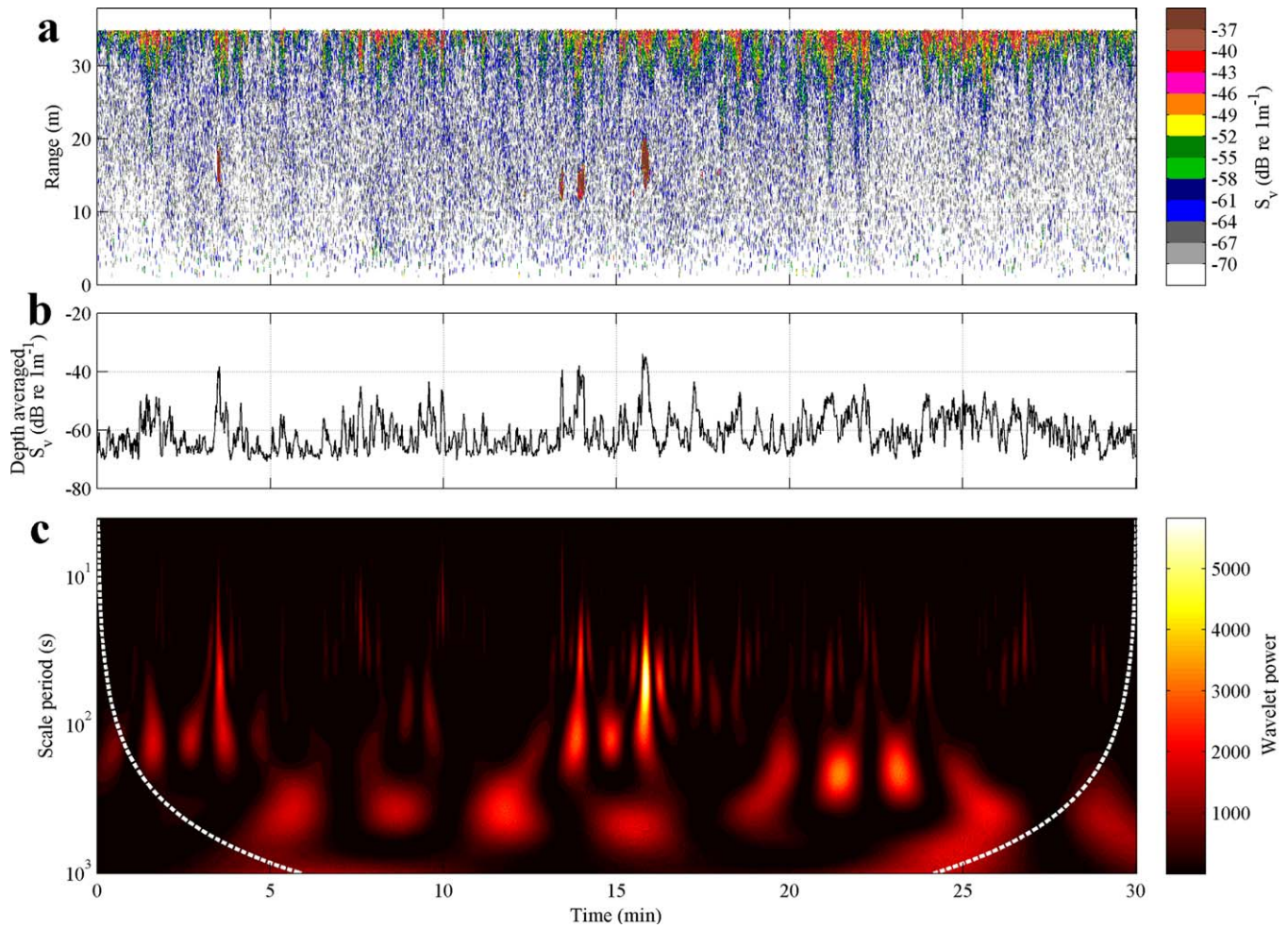


Fig. 4. Wavelet analysis on short-scale backscatter features. **(a)** Echogram from the Fall of Warness showing 30 min of $S_{v200\text{clean}}$ data containing clear fish school targets and moderate near-surface turbulence. **(b)** Depth averaged S_v time series for the data in **(a)**. **(c)** Wavelet power spectrum for **(b)** showing dominant scales in the time domain. The non-stationary S_v contributions from fish schools give intermittent features at shorter scales than the dominant physical scales which dominate global power spectra; however, there is clear scale overlap with some turbulent backscatter. The white dashed line indicates the cone of influence where edge effects of the finite-length time series analyzed are significant.

bodies, such as fish aggregations (e.g., Fig. 1), and so the median gives superior performance. The median is calculated and assigned to the central element of each overlapping window to give the smoothed representation of the broad backscatter conditions. Elements in the window which extend beyond the available data array or have been excluded during previous processing steps are not included in calculating the median. Selection of the appropriate window dimensions for calculating the median is critical to the effectiveness of this step and must be adjusted for the site dynamics and targets of interest.

Through wavelet analysis insights and subsequent iterative experimentation, a moving window of five elements in the vertical (0.95 m in range) and 135 elements in the horizontal (135 s in time) was selected. A window as small as possible is desirable to effectively resolve the physical backscatter variations. However, the horizontal dimension should be at least

twice the time persistence of the largest targets in the dataset so that the median does not reflect backscatter characteristics of targets of interest. Similarly, the vertical dimension should be small enough so that the full vertical behavior of the background conditions is well resolved while still providing effective smoothing performance. Since in the data here the largest targets are fish schools persisting for around 1 min and vertical trends are relatively stable within 1 m (Fig. 1), the 5×135 median window operation gives effective performance in this case. This operation is performed on the $S_{v200\text{clean}}$ data to give $S_{v5 \times 135}$ as shown in Fig. 5.

To remove long-scale contributions to $S_{v200\text{clean}}$ the data samples are selectively modified when the $S_{v5 \times 135}$ matrix exceeds the threshold, λ . This threshold is set for the conditions where false target detection occurs due to elevated levels of backscatter. This of course depends on the acoustic properties of the targets of interest and ultimately the

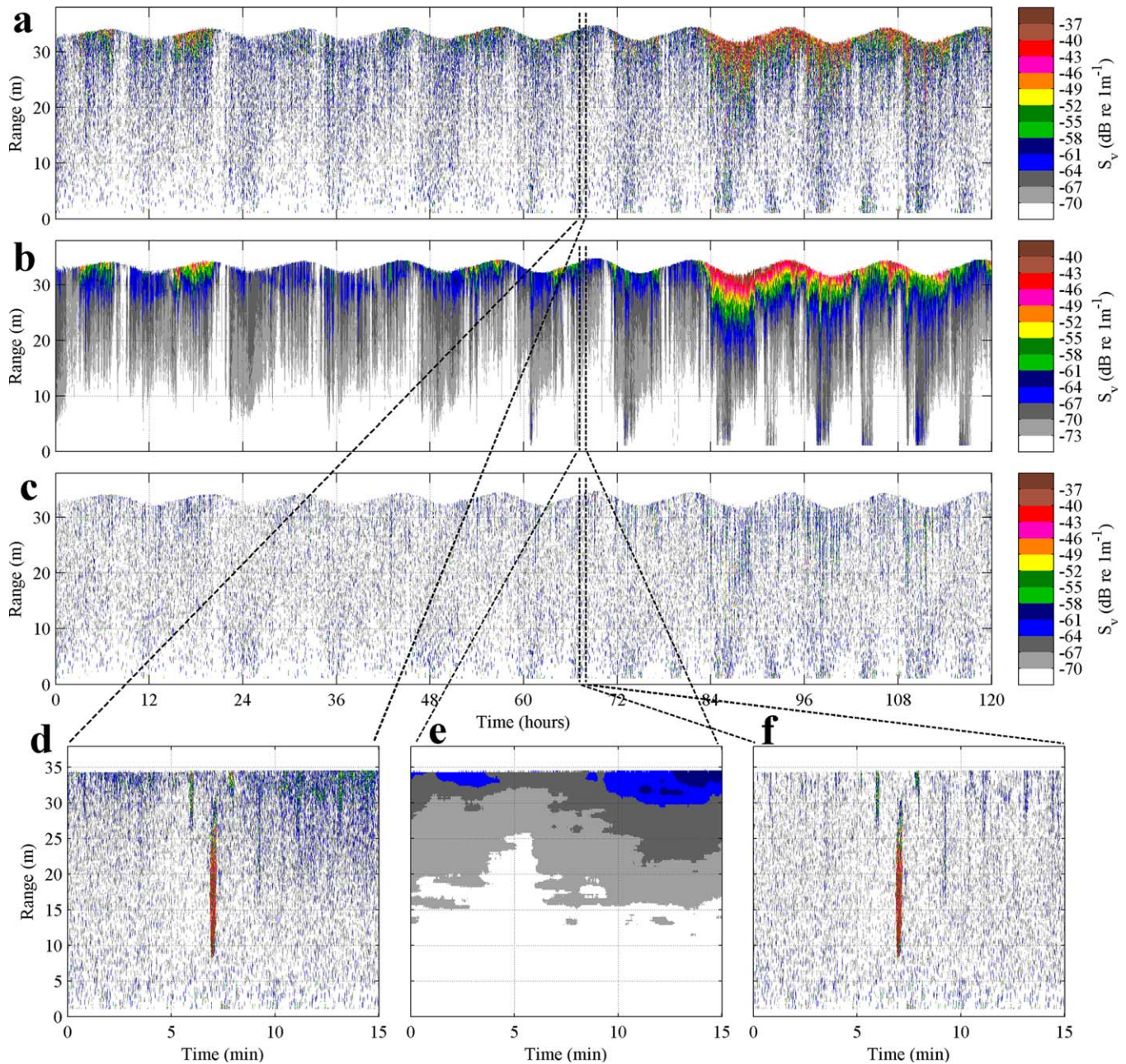


Fig. 5. Smoothing and suppression using moving window operator. **(a)** Five days of continuous $S_{V200\text{clean}}$ data recorded at the Fall of Warness. Broad variations in backscatter are apparent relating to the changing tidal and meteorological conditions. **(b)** Median smoothed data using a 5×135 window gives $S_{V5 \times 135}$ data which represents the long-scale backscatter contributions due to the physical dynamics without including biological targets. **(c)** Selective subtraction of **(b)** from **(a)** gives the stabilized data set $S_{V\text{ suppress}}$ which forms the basis of subsequent processing. Long-scale trends are removed when necessary leaving only backscattering structures at the scales of interest. **(d)** Detail of **(a)** showing large fish school. **(e)** Detail of **(b)** showing the same section as **(d)**, the broad physical variations in backscatter are well resolved, however, crucially the fish school is not represented forming the basis of scale selectivity. **(f)** Detail of **(c)** showing the same section shown in **(d)** with target unaffected but broad trends in depth and time suppressed.

detection thresholds applied to the modified data. For the isolation of targets shown in the following sections and figures λ is set at -73 dB following iterative experimentation with the desired detection thresholds, and the suppression process works for each available data sample as follows:

$$S_{V5 \times 135} \leq \lambda \rightarrow S_{V\text{ suppress}} = S_{V\text{ clean}} \quad (1)$$

$$S_{V5 \times 135} > \lambda \rightarrow S_{V\text{ suppress}} = S_{V\text{ clean}} - S_{V5 \times 135} + \lambda \quad (2)$$

As demonstrated in Fig. 5, this selective suppression effectively stabilizes long-scale trends in depth and time to give

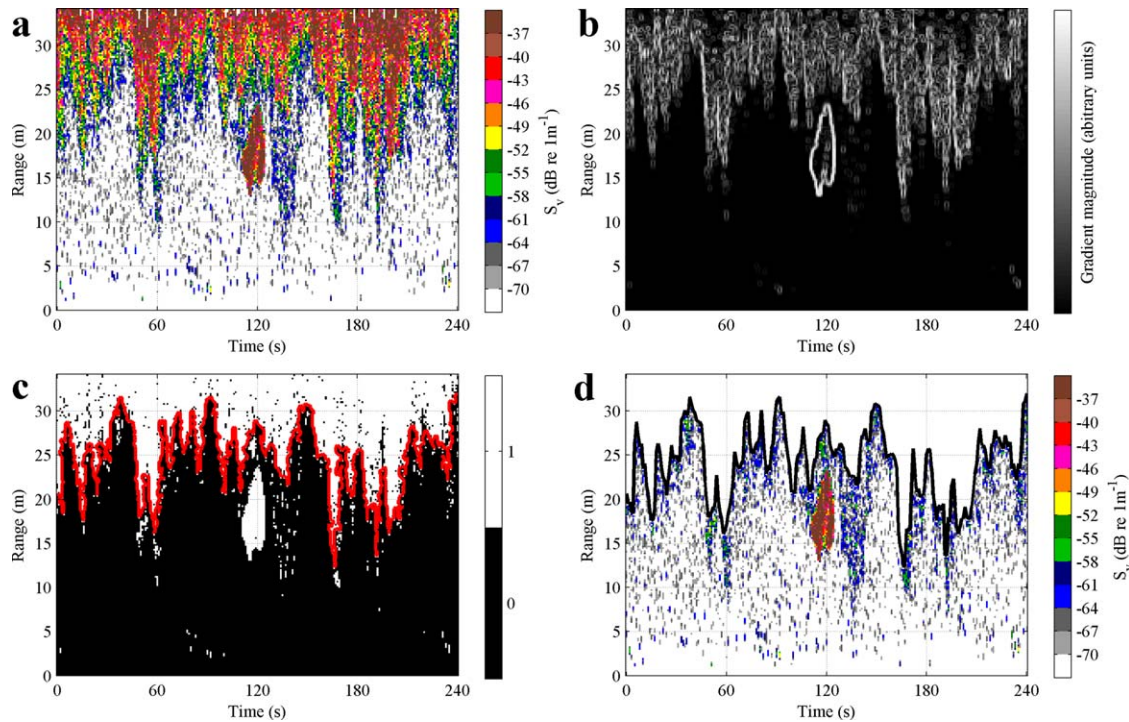


Fig. 6. Morphological filtering approaches to exclude short-scale turbulent backscatter in the near surface. **(a)** Section of $S_{V200clean}$ data showing intense near-surface turbulence and fish school. **(b)** The gradient magnitude computed using a Sobel filter for each data point for visualizing and specifying turbulent structures and target boundaries. **(c)** Binary image generated by alternative thresholding approach, connectivity to the sea surface boundary defines the turbulence boundary shown in red. **(d)** Turbulence exclusion gives $S_{V\ morph}$ data, the range to turbulent structures z_{turb} is shown in black and defined by the minimum value per ping for the red line in **(c)**.

$S_{V\ suppress}$ data. Target detection on $S_{V\ suppress}$ data would show much better performance using standard S_V and size thresholding methods for target detection by still giving sensitivity to strong targets in high backscatter conditions ($>\lambda$) without reducing sensitivity during low backscatter conditions ($\leq\lambda$). However, some false targets will still persist where turbulent backscattering structures are of a comparable scale to the targets of interest. The removal of these features motivates the use of additional filters based on morphological characteristics as described below.

Morphological filtering

The previous processing step will not mitigate the effects of turbulent backscattering features that are of a comparable scale to the targets of interest. In particular, vertical mixing can drive wave generated clouds of air bubbles from the near surface into extended intense backscattering structures which can vary over short timescales. These features must be excluded from analysis or false targets will still be present and so an additional filter is required. Intense turbulent structures are morphologically isolated based on their connectivity with physical boundaries (e.g., the sea surface) and again an optimal threshold is derived to exclude the minimum data possible from further analysis. Tracing algorithms

generate detailed boundary lines for these intense physical backscattering structures which are used to remove them from further target detection steps.

Effective morphological exclusion is challenging when targets are within or close to boundaries or intense turbulence (e.g., Fig. 6). Various edge detection algorithms were explored to exclude short-scale turbulent structures without the loss of genuine targets. A promising approach is the use of a backscatter gradient metric to delineate turbulence and targets based on the first derivative of S_V values. To assign a gradient value to each S_V element a Sobel filter is a useful isotropic discrete differentiation operator with minimum smoothing which uses two weighted 3×3 kernels to compute the first derivative around each pixel (Petrou and Petrou 2010). This filter can be applied to a section of data to characterize boundaries in the echogram by the absolute gradient (Fig. 6).

Simple line-picking and tracing algorithms based on some threshold are readily available in echosounder processing applications and can also be used to identify turbulent boundaries with reasonable effectiveness. However, intense near-surface turbulence can form complex arcing structures which confound methods designed to identify a simple surface. Instead, using a threshold defined binary representation

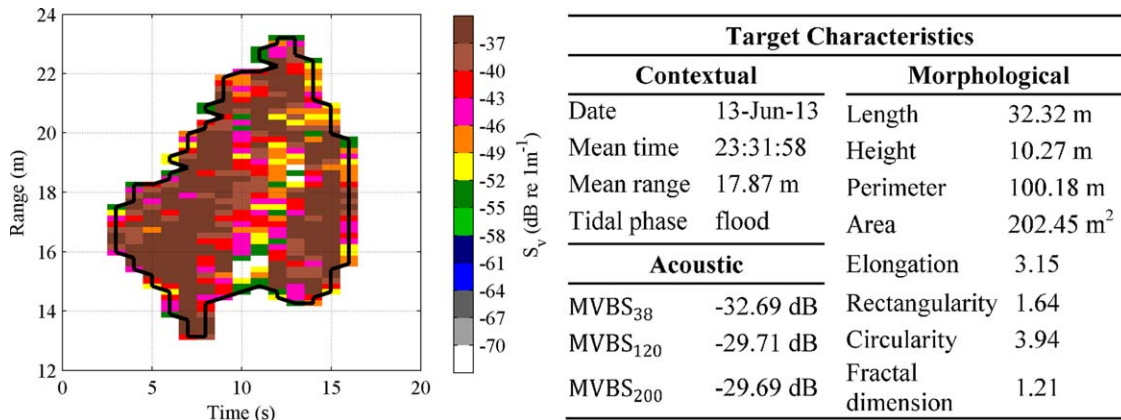


Fig. 7. Target delineation and characterization of the fish school shown in Fig. 6. The image shows the thresholded S_v stable data used to define the target boundary highlighted by the black line. Some simple target characteristics are presented which are used for target validation and characterization. Acoustic properties are computed using S_v clean data and morphological characteristics follow the definitions given in Korneliussen et al. (2009).

of the data to define complex boundaries with high resolution gives improved performance (Fig. 6). Here we calculate an optimal threshold of -59 dB in the same manner as for the sea surface detection (Otsu 1975) for minimal data exclusion. This approach is used to define a boundary line by the minimum range to turbulent structures (z_{turb}) which is the basis of morphological exclusion based on connectivity of intense backscatter to a boundary (here the sea surface) to give S_v morph.

Samples removed by the morphological exclusion in S_v morph are also removed from the scale selective filtering results in S_v suppress to give a processed data version (S_v stable), appropriate for standard target detection methodologies. This stabilized data version has mitigated the overwhelming effects of long-scale variations in the background acoustic conditions and short-scale intense turbulent structures so that biological targets are now clearly identifiable.

Target delineation

Target detection is performed on the S_v stable data using S_v and area thresholds. The thresholds depend on the acoustic characteristics of the target of interest. For the detection of fish, such as aggregations of gadoids and clupeids, we use a -55 dB threshold for each pixel and a minimum 10 pixel connected region to identify a target. These requirements represent a sufficiently cautious S_v threshold (Burgos and Horne 2007) and sensitivity to small aggregations, while still providing a useful number of pixel samples for the characterization of each target. To maintain the highest resolution and identify small targets where possible, no connectivity criterion is specified and no amalgamation operation is performed.

The target boundaries derived from the processed data are overlain onto the S_v clean data for each frequency to extract acoustic properties from unmodified backscatter data. Independent concurrent model flow velocity information for the

site is used to transform target persistence (time) into approximate target length (distance) by the simple multiplication of depth-averaged flow speed with the length of time each target is present. The mean volume backscattering strength (MVBS) is calculated for each frequency over all pixels which pass the S_v threshold within each target. Target MVBS values are computed by taking the logarithm of the averaged linear expressions of target pixel S_v values. Various other acoustic, statistical, morphological, and contextual characteristics are computed for each target in line with the definitions in Korneliussen et al. (2009) and Horne (2000). These characteristics form the basis of subsequent validation, characterization, and analysis. The target delineation process and some selected simple target characteristics are presented in Fig. 7 for the fish school shown in Fig. 6.

Target validation

The validation of targets ensures that chosen discriminating characteristics are in the range of values expected from prior knowledge. This step is again particular to the nature of the targets of interest. For example, frequency differencing is a common technique for the isolation of particular fish species (Kloser et al. 2002; Logerwell and Wilson 2004). Similarly, contextual and morphological characteristics relevant to specific behavior can also be used in species identification approaches. However, these characteristics have been shown to vary with location, depth, age, and season and so caution must be exercised when making direct comparisons to target characteristics made in relatively stable aquatic environments to the characteristics recorded in the turbulent and highly dynamic environments discussed here. Nonetheless some intrinsic physical properties of targets are comparable and so effective target validation is possible.

Taking the isolation of fish schools as an example, we can set theoretical limits on the frequency difference, $\Delta MVBS$ (e.g., $MVBS_{200} - MVBS_{38}$), which we anticipate given known

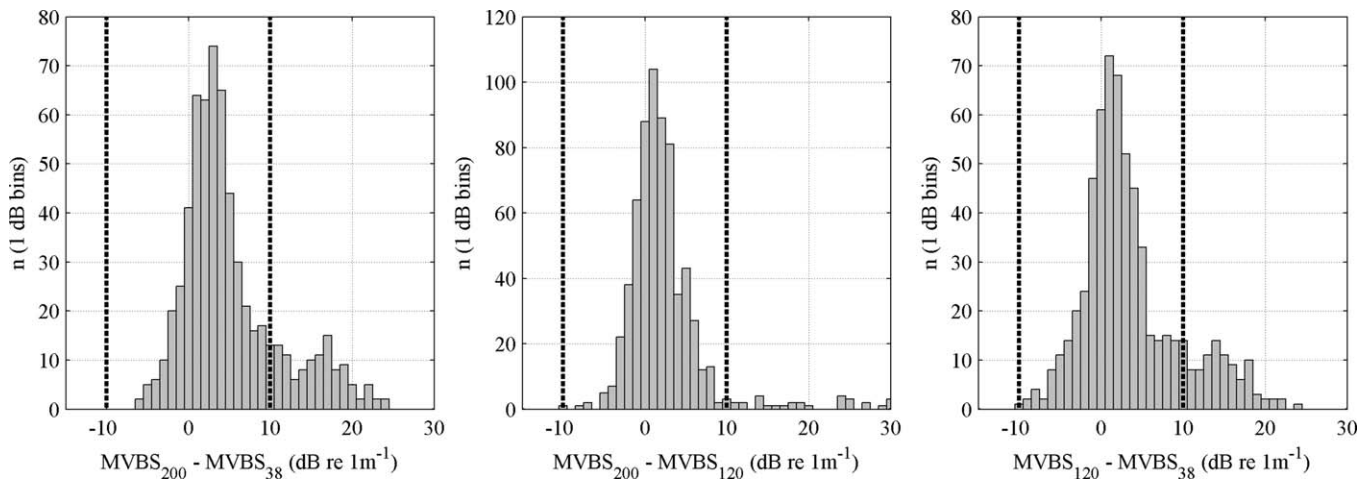


Fig. 8. Multifrequency validation of detected targets using frequency differencing. The number (n) of targets is shown in 1 dB bins. The $\Delta MVBS$ is calculated for each frequency combination to inspect frequency response characteristics. As fish are anticipated to have relatively low $\Delta MVBS$ then targets are validated based on the tolerated frequency band ($-10 \text{ dB} < \Delta MVBS < 10 \text{ dB}$) highlighted by the thick black dashed lines. As fish schools are the dominant targets using these detection settings then the majority are validated.

physical properties (such as size and composition) of the targets of interest. Small objects, such as air bubbles and plankton, can have a high variation in S_v over the frequencies used here due to size-dependent Rayleigh and resonant scattering effects (Lavery et al. 2007). In contrast, the frequency response of fish species at the frequencies used here is dominated by simple geometric backscatter and is relatively constant (Kang et al. 2002). Therefore, we can validate potential fish school targets by inferring target identity from the observed frequency differences. Frequency difference results for all targets using the detection thresholds described above (-55 dB and 10 connected pixels) for a platform deployment are presented in Fig. 8.

As we are not aiming to isolate just one particular species of fish we tolerate a relatively large frequency difference band ($-10 \text{ dB} < \Delta MVBS < 10 \text{ dB}$) similar to the range used for fish isolation in Benoit-Bird et al. (2011). This can be adjusted and made more specific to isolate more specific taxa bearing in mind the uncertain nature of target characteristics in the site. If any available $\Delta MVBS$ results for each detected target are beyond the tolerated frequency band they are rejected as false targets attributed to small scatterers such as plankton or the spurious inclusion of air bubbles or suspended sediment. The majority of targets are accepted in this case, which is desirable given the wide range of target species of interest and turbulence mitigation steps. The frequency combinations of $MVBS_{200} - MVBS_{38}$ and $MVBS_{120} - MVBS_{38}$ are generally used in frequency difference work (Kang et al. 2002; Korneliussen et al. 2009; Benoit-Bird et al. 2011; Sato et al. 2015) as 38 kHz data can include significant resonant effects for small scatterers, and consequently demonstrate higher variation in the results here (Fig. 8). However, in our case the $MVBS_{200} - MVBS_{120}$ comparison is

also important as it provides validation for targets within the 38 kHz near field (i.e., between the ranges of 2.1 m and 6.3 m). The results of this validation form the basis of subsequent assessment and discussion.

Assessment

The proposed target detection method was applied to the available data from both 2013 platform deployments at the Fall of Warness. Using the processing, detection, and validation parameters described above, 523 fish schools were identified in the first deployment and 396 fish schools in the second. Each individual target was inspected manually with reference to the raw data and the effectiveness of the method was demonstrated for all conditions encountered. This is shown for 6 d of continuous data during highly variable conditions in Fig. 9 demonstrating the effectiveness and flexibility of the method. Visualizing targets is difficult at the long-time scales where physical variations are clear, however, reference to a shorter data section (both processed and unprocessed) and details of individual targets demonstrates the variety of conditions encountered during processing.

The clear variation in target characteristics and behaviors further highlights the flexibility of this method. Targets are identifiable at all depths within the water column and throughout the entire datasets. This is visible from the target distributions and bar charts in Fig. 9. Without turbulence mitigation measures, then false targets dominate detections and bias results during enhanced backscatter. However, following the processing there is no apparent bias remaining during turbulent sections compared with calm sections and there are consistent behavioral differences observed between flow directions and deployments regardless of the acoustic

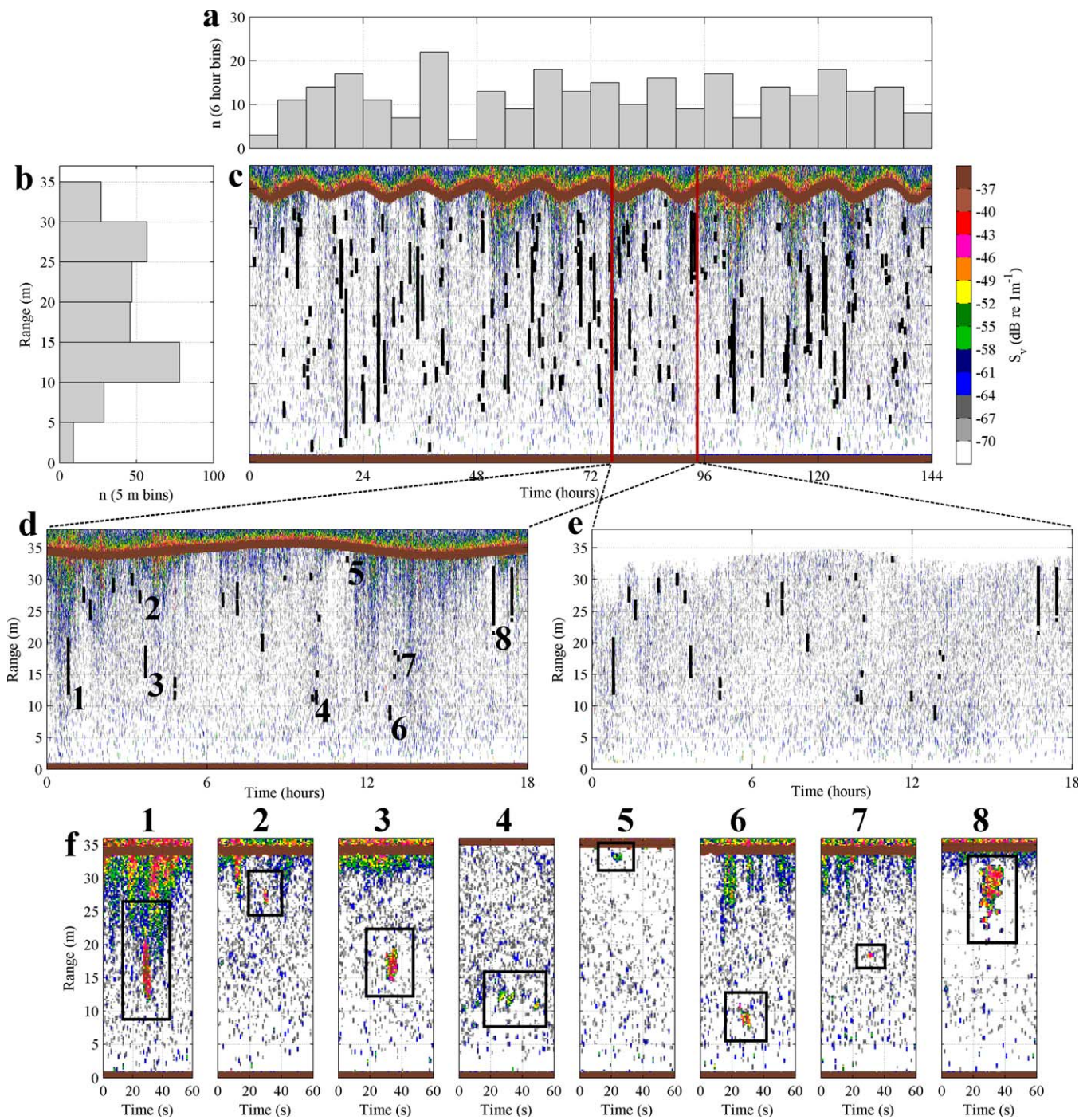


Fig. 9. Target detection and distributions over varying physical conditions. Data are from a continuous 6-d section at the Fall of Warness during mixed meteorological conditions and varying tidal dynamics. (a) The temporal distribution of targets shows natural variation but no strong correlation with the background physical conditions demonstrating that processing has been successful with no contributions from false targets. (b) The depth distribution of targets binned by their mean range demonstrates successful detection throughout the water column and gives behavioral information on their depth preference. (c) The full data section shown as unprocessed S_{v200} data with target boundaries overlain in black lines. The vast majority of visible backscatter is of physical origin and particularly intense in the near surface environment. Although this scale is too broad to make out individual target characteristics the overall target distribution through the changing conditions is clear. (d) Expanded sub-section showing target distribution in black on unprocessed S_{v200} data. (e) The same sub-section as (d) with target distributions overlain in black but on processed $S_{v\text{ stable}}$ data which is the basis of target delineation and demonstrates the effectiveness of turbulence mitigation measures. (f) Details for selected targets labeled in (d) shown in S_{v200} data demonstrating a variety of local physical conditions and target characteristics. Rather than plotting target boundaries at this scale which would obscure target edge pixels the detected targets are highlighted in the center of a black box.

conditions. The morphological filtering process excludes only 2.4% of data during this section, suggesting that any potential effect on target results is limited and demonstrating a substantial improvement to data coverage compared with many existing approaches. Detected targets vary from large schools occupying most of the water column for up to a minute, to small targets only occupying a few pings at a very specific depth. Schools are often spatially well-defined with high *MVBS*; however, less well-defined aggregations with lower *MVBS* are also detected and validated. This range of target behavior and acoustic properties demonstrates the sensitivity of this method even with relatively conservative thresholds.

The processing steps used depend on custom made adaptive filters and line picking algorithms to facilitate the use of standard detection criteria on highly unstable data. However, similar tools available in echosounder analysis packages (e.g., Echowiew) can be adapted to emulate these methods and so this approach could be followed by a wide range of users with minimal difficulty. None of the above processing algorithms are inhibitive computationally expensive, and exporting the S_V stable data facilitates the use of conventional target detection and analysis methods. Applying more specific validation requirements allows for the isolation of certain species or target types.

Success of this method depends on optimized processing and detection thresholds which are specific to the targets of interest and dynamics of the site. The isolation of particular scales depends on considering some maximum target size which separates ecological contributions to backscatter from long-scale physical sources. As a result, this technique is not appropriate for continuous layers of targets. Due to the connectivity requirements for morphological filtering, detection is also limited within the most intense turbulence structures and for strong targets with no separation from the surface. With the impracticality of obtaining comparative direct biological sampling information the quality control for this paper is undertaken by direct scrutiny of each target.

This method successfully addresses the challenge of reliable target detection across dynamic physical conditions. Without the novel turbulence mitigation steps then sensitive target detection results are overwhelmed by false targets during turbulent sections. Similarly, simply increasing detection thresholds to attempt to exclude turbulent backscatter would remove the vast majority of genuine targets and still fail to differentiate intense turbulence structures from large fish schools. With reference to the targets highlighted in Fig. 9, it is clear that existing approaches which use standard target detection methods on data with severe restriction in depth or temporal coverage would lead to substantial losses of data and the introduction of sampling bias. This method introduces a new approach which is flexible through time, depth, and for a wide variety of target characteristics.

Discussion

Reliable active acoustic monitoring in turbulent environments is an essential requirement for understanding ecological dynamics in a variety of aquatic environments. In particular, the recent international progress in marine renewable energy technologies has made robust target detection in tidal channels a priority for the consenting and environmental impact assessment for the operation of marine energy devices. Such sites demonstrate extreme spatial and temporal variations in physically generated backscatter with changes in the meteorological conditions and tidal dynamics. This leads to highly unstable acoustic conditions and the failure of standard target detection algorithms used in fisheries acoustics.

Existing methods require substantial compromises in data quality or coverage, or depend on intensive and subjective human scrutiny. The method presented here improves on standard techniques by adaptive processing which ensures high detection sensitivity and data coverage without the inclusion of false targets or removal of genuine targets. For example, previous methods would not detect some of the small and shallow aggregations detectable by this method which can have significant ecological importance for some species such as shallow diving seabirds (Speckman 2004). Similarly, some previous methods would include substantial contributions from false targets during turbulent sections leading to the misinterpretation of ecological distributions and interactions.

The method proposed here isolates biological targets from physical interference; however, there are still limitations to this approach which mean that it is unlikely that every potential target is detected. For example, there is no target information at ranges less than 2.1 m due to near field effects inherent to the acoustic system used here. Similarly, potential targets that are not morphologically discernable from the most intense turbulent structures would be lost in the small proportion of data that are excluded. Given the thresholds and processing parameters used here, it is unlikely that individual fish or highly dispersed aggregations would be detected.

Detection thresholds and processing parameters are set according to the nature of the targets of interest and the site dynamics. Crucially, since this approach is automatic the results are completely repeatable and so this method is an important tool for comparative studies in turbulent environments. Such comparisons are vital for the quantitative assessment of site characteristics and for systematically establishing the significance of human impacts. In the application considered here, comparison of data from different platform deployments can provide detailed information on target distributions and interactions in high energy marine sites and around marine renewable energy infrastructure. Such comparisons can provide information needed for

environmental impact assessment of marine energy technologies, such as evidence of the displacement or attraction of fish species. Such evidence has implications for the foraging behavior of predators and associated risks to these species which require quantification for project consenting.

In general, independent verification of acoustic results is often provided by direct sampling techniques which are impractical in high energy sites such as the tidal channel studied here. This provides an additional difficulty in target detection as there is a lack of reference data to guide target composition approximations and species differentiation. These limitations are accepted in this method by isolating targets by inherent physical properties and broad validation criteria based on multifrequency characteristics. Although this method is automatic, assessing success for this paper is dependent on manual inspection and scrutiny to verify target distribution results.

Although the emphasis here has been on the detection of fish schools, the proposed method can be extended to other types of targets. For example diving seabirds and their bubble trails can be detected using multifrequency echosounders (e.g., Benoit-Bird et al. 2011), and are visible in the data presented here and confirmed by synchronized multibeam measurements showing clear bird diving tracks (Williamson et al. In press). However, the number of confirmed bird dives identified so far is too low to develop an optimized detection approach. Nonetheless, the same approach used for fish detection is functional combined with specific validation requirements. Example bird bubble trail validation requirements are a narrow $\Delta MVBS$ band (substantially higher backscatter was observed in 38 kHz data by Benoit-Bird et al. 2011) and characteristic morphological parameter such as low elongation. Similar target specific validation requirements could be established for marine mammal identification.

The outputs of this method provide information from data which could otherwise be misinterpreted or discarded. Such target results are essential for the environmental impact assessment of emerging marine energy technologies, and provide vital information on ecological interactions and distributions in important environments with growing industrial importance.

Comments and recommendations

Successful implementation of this method, like almost any method, depends on carefully selected processing parameters to optimize performance. A reduction in performance is likely to lead to the loss of sensitivity or inclusion of false targets and therefore inspection of processing results throughout is essential. It is recommended to check closely in both highly turbulent and relatively calm data sections with reference to particularly challenging targets. Further reference to S_v histograms and statistics, as shown, is also

advised. Insights from power spectra and wavelet analysis can further accelerate processing and verification of results.

The concepts of scale-dependent adaptive filtering and morphological exclusion can be readily applied to different instruments and in different contexts. In the case of multi-beam echosounder and acoustic camera data then scale isolation by applying a smoothing window through both time and space for adaptive suppression will reduce false target detections and increase sensitivity for target tracking algorithms. Application of this approach for multibeam monitoring around marine renewable infrastructure is the subject of ongoing work. Similarly, these methods can be independent of multifrequency information, and with a limited reduction in sensitivity, can be applied to single frequency echosounder datasets. Increasingly used broadband echosounder systems are also compatible with this approach given appropriate refinements to the multifrequency validation process. While this method has been designed for the detection of fish in tidal channels, the flexibility of the tools described in this paper may enable the analysis of turbulent data from many other potential applications.

References

- Barange, M. 1994. Acoustic identification, classification and structure of biological patchiness on the edge of the Agulhas Bank and its relation to frontal features. *S. Afr. J. Mar. Sci.* **14**: 333–347. doi:10.2989/025776194784286969
- Baussant, T., F. Ibanez, and M. Étienne. 1993. Numeric analysis of planktonic spatial patterns revealed by echograms. *Aquat. Living Resour.* **6**: 175–184. doi:10.1051/alr:1993019
- Benjamins, S., A. C. Dale, G. Hastie, J. J. Waggitt, M. A. Lea, B. E. Scott, and B. Wilson. 2015. Confusion reigns? A review of marine megafauna interactions with tidal-stream environments. *Oceanogr. Mar. Bio: Annu. Rev.* **53**: 1–54. doi:10.1201/b18733-2
- Benoit-Bird, K. J., K. Kuletz, S. Heppell, N. Jones, and B. Hoover. 2011. Active acoustic examination of the diving behavior of murrets foraging on patchy prey. *Mar. Ecol. Prog. Ser.* **443**: 217–235. doi:10.3354/meps09408
- Bertrand, A., and others. 2008. Schooling behaviour and environmental forcing in relation to anchoveta distribution: An analysis across multiple spatial scales. *Prog. Oceanogr.* **79**: 264–277. doi:10.1016/j.pocean.2008.10.018
- Burgos, J. M., and J. K. Horne. 2007. Sensitivity analysis and parameter selection for detecting aggregations in acoustic data. *J. Mar. Sci.* **64**: 160–168. doi:10.1093/icesjms/fsl007
- Cazelles, B., M. Chavez, D. Berteaux, F. Ménard, J. O. Vik, S. Jenouvrier, and N. C. Stenseth. 2008. Wavelet analysis of ecological time series. *Oecologia* **156**: 287–304. doi:10.1007/s00442-008-0993-2
- Crawford, G. B., and D. M. Farmer. 1987. On the spatial distribution of ocean bubbles. *J. Geophys. Res: Oceans* **92**: 8231–8243. doi:10.1029/jc092ic08p08231

- Deane, G. B., J. C. Preisig, and A. C. Lavery. 2013. The suspension of large bubbles near the sea surface by turbulence and their role in absorbing forward-scattered sound. *IEEE J. Oceanic Eng.* **38**: 632–641. doi:[10.1109/joe.2013.2257573](https://doi.org/10.1109/joe.2013.2257573)
- Donoho, D. L. 1995. De-noising by soft-thresholding. *IEEE Trans. Inf. Theory.* **41**: 613–627. doi:[10.1109/18.382009](https://doi.org/10.1109/18.382009)
- Foote, K., H. Knudsen, G. Vestnes, D. Maclennan, and E. Simmonds. 1987. Calibration of acoustic instruments for fish density estimation: A practical guide. *ICES Coop. Res. Rep.* **144**: 1–69.
- Horne, J. K. 2000. Acoustic approaches to remote species identification: A review. *Fish. Oceanogr.* **9**: 356–371. doi:[10.1046/j.1365-2419.2000.00143.x](https://doi.org/10.1046/j.1365-2419.2000.00143.x)
- Jacques, D. A. 2014. Describing and comparing variability of fish and macrozooplankton density at marine hydrokinetic energy sites. M.Sc. thesis. Univ. of Washington.
- Jacques, D. A., and J. K. Horne. 2014. Scaling of spatial and temporal biological variability at marine renewable energy sites. *In Proceedings of the Second Marine Energy Technology Symposium (METS2014)*, Seattle, USA, 15-18 April 2014.
- Joslin, J., B. Polagye, and A. Stewart. 2014. Development of an adaptable monitoring package for marine renewable energy. *In Proceedings of the Fifth International Conference on Ocean Energy (ICOE2014)*, Halifax, Canada, 4-6 November 2014.
- Kang, M., M. Furusawa, and K. Miyashita. 2002. Effective and accurate use of difference in mean volume-backscattering strength to identify fish and plankton. *ICES J. Mar. Sci.* **59**: 794–804. doi:[10.1006/jmsc.2002.1229](https://doi.org/10.1006/jmsc.2002.1229)
- Kloser, R. J., T. Ryan, P. Sakov, A. Williams, and J. A. Koslow. 2002. Species identification in deep water using multiple acoustic frequencies. *Can. J. Fish. Aquat. Sci.* **59**: 1065–1077. doi:[10.1139/f02-076](https://doi.org/10.1139/f02-076)
- Korneliussen, R. J., Y. Heggelund, I. K. Eliassen, and G. O. Johansen. 2009. Acoustic species identification of schooling fish. *ICES J. Mar. Sci.* **66**: 1111–1118. doi:[10.1093/icesjms/fsp119](https://doi.org/10.1093/icesjms/fsp119)
- Lavery, A. C., R. W. Schmitt, and T. K. Stanton. 2003. High-frequency acoustic scattering from turbulent oceanic microstructure: The importance of density fluctuations. *J. Acoust. Soc. Am.* **114**: 2685–2697. doi:[10.1121/1.1614258](https://doi.org/10.1121/1.1614258)
- Lavery, A. C., P. H. Wiebe, T. K. Stanton, G. L. Lawson, M. C. Benfield, and N. Copley. 2007. Determining dominant scatterers of sound in mixed zooplankton populations. *J. Acoust. Soc. Am.* **122**: 3304–3326. doi:[10.1121/1.2793613](https://doi.org/10.1121/1.2793613)
- Logerwell, E. A., and C. D. Wilson. 2004. Species discrimination of fish using frequency dependent acoustic backscatter. *ICES J. Mar. Sci.* **61**: 1004–1013. doi:[10.1016/j.icesjms.2004.04.004](https://doi.org/10.1016/j.icesjms.2004.04.004)
- Lu, Y., R. G. Lueck, and D. Huang. 2000. Turbulence characteristics in a tidal channel. *J. Phys. Oceanogr.* **30**: 855–867. doi:[10.1175/1520-0485\(2000\)030<0855:tciatc>2.0.co;2](https://doi.org/10.1175/1520-0485(2000)030<0855:tciatc>2.0.co;2)
- Melvin, G. D., and N. A. Cochrane. 2015. Multibeam acoustic detection of fish and water column targets at high-flow sites. *Estuar. Coast.* **38**: 227–240. doi:[10.1007/s12237-014-9828-z](https://doi.org/10.1007/s12237-014-9828-z)
- Moum, J. N., D. M. Farmer, W. D. Smyth, L. Armi, and S. Vagle. 2003. Structure and generation of turbulence at interfaces strained by internal solitary waves propagating shoreward over the continental shelf. *J. Phys. Oceanogr.* **33**: 2093–2112. doi:[10.1175/15200485\(2003\)033<2093:sagota>2.0.co;2](https://doi.org/10.1175/15200485(2003)033<2093:sagota>2.0.co;2)
- Nero, R. W., and J. J. Magnuson. 1989. Characterization of patches along transects using high resolution 70-kHz integrated acoustic data. *Can. J. Fish. Aquat. Sci.* **46**: 2056–2064. doi:[10.1139/f89-254](https://doi.org/10.1139/f89-254)
- Ona, E., and M. Barange. 1999. Single target recognition. *ICES Coop. Res. Rep.* **235**: 28–43.
- Otsu, N. 1975. A threshold selection method from gray-level histograms. *IEEE Trans. Syst. Man Cybern.* **9**: 62–66. doi:[10.1109/0018-9472/79/0100-0062](https://doi.org/10.1109/0018-9472/79/0100-0062)
- Petrou, M., and C. Petrou. 2010. *Image processing: The fundamentals*, 2nd ed. Wiley, p. 794.
- Plueddemann, A. J., J. A. Smith, D. M. Farmer, R. A. Weller, W. R. Crawford, R. Pinkel, S. Vagle, and A. Gnanadesikan. 1996. Structure and variability of Langmuir circulation during the Surface Waves Processes Program. *J. Geophys. Res: Oceans* **101**: 3525–3543. doi:[10.1029/95JC03282](https://doi.org/10.1029/95JC03282)
- Polagye, B., A. Copping, R. Suryan, S. Kramer, J. Brown-Saracino, and C. Smith. 2014. Instrumentation for monitoring around marine renewable energy converters. Workshop final report. PNNL-23110 Pacific Northwest National Laboratory.
- Reid, D., C. Scalabrin, P. Petitgas, J. Masse, R. Aukland, P. Carrera, and S. Georgarakos. 2000. Standard protocols for the analysis of school based data from echo sounder surveys. *Fish. Res.* **47**: 125–136. doi:[10.1016/S0165-7836\(00\)00164-8](https://doi.org/10.1016/S0165-7836(00)00164-8)
- Sato, M., J. K. Horne, S. L. Parker-Stetter, and J. E. Keister. 2015. Acoustic classification of coexisting taxa in a coastal ecosystem. *Fish. Res.* **172**: 130–136. doi:[10.1016/j.fishres.2015.06.019](https://doi.org/10.1016/j.fishres.2015.06.019)
- Scott, B. E., R. Langton, E. Philpott, and J. J. Waggitt. 2014. Seabirds and marine renewables: Are we asking the right questions?, p. 81–92. *In* M. A. Shields and A. I. L. Payne [eds.], *Marine renewable energy technology and environmental interactions*. Springer.
- Simmonds, J., and D. N. MacLennan. 2005. *Fisheries acoustics: Theory and practice*, 2nd ed. Blackwell Science, p. 437.
- Speckman, S. G. 2004. Characterizing fish schools in relation to the marine environment and their use by seabirds in lower Cook Inlet, Alaska. Ph.D. thesis. Univ. of Washington.
- Staines, G., G. Zydlewski, H. Viehman, H. Shen, and J. McCleave. 2015. Changes in vertical fish distributions near a hydrokinetic device in Cobscook Bay, Maine, USA. *In Proceedings of the 11th European Wave and Tidal*

- Energy Conference (EWTEC2015), Nantes, France, 6-11 September 2015.
- Thomson, J., B. Polagye, V. Durgesh, and M. C. Richmond. 2012. Measurements of turbulence at two tidal energy sites in Puget Sound, WA. *IEEE J. Oceanic Eng.* **37**: 363–374. doi:10.1109/joe.2012.2191656
- Thorne, P. D., and D. M. Hanes. 2002. A review of acoustic measurement of small-scale sediment processes. *Cont. Shelf Res.* **22**: 603–632. doi:10.1016/S0278-4343(01)00101-7
- Torrence, C., and G. P. Compo. 1998. A practical guide to wavelet analysis. *Bull. Amer. Meteor. Soc.* **79**: 61–78. doi:10.1175/1520-0477(1998)079<0061:apgtwa>2.0.co;2
- Trevorrow, M. V. 1998. Boundary scattering limitations to fish detection in shallow waters. *Fish. Res.* **35**: 127–135. doi:10.1016/S0165-7836(98)00067-8
- Viehman, H. A., and G. B. Zydlewski. 2014. Fish interactions with a commercial-scale tidal energy device in the natural environment. *Estuar. Coast.* **38**: 241–252. doi:10.1007/s12237-014-9767-8
- Viehman, H. A., G. B. Zydlewski, J. D. McCleave, and G. J. Staines. 2014. Using hydroacoustics to understand fish presence and vertical distribution in a tidally dynamic region targeted for energy extraction. *Estuar. Coast.* **38**: 215–226. doi:10.1007/s12237-014-9776-7
- Viehman, H., and G. B. Zydlewski. 2015. Using temporal analysis techniques to optimize hydroacoustic surveys of fish at MHK devices. *In Proceedings of the 11th European Wave and Tidal Energy Conference (EWTEC2015)*, Nantes, France, 6-11 September 2015.
- Waggitt, J. J., P. W. Cazenave, R. Torres, B. J. Williamson, and B. E. Scott. 2016. Quantifying pursuit-diving seabirds' associations with fine-scale physical features in tidal stream environments. *J. App. Ecol.* **53**: 1653–1666. doi:10.1111/1365-2664.12646
- Wiesebron, L. E. 2015. Evaluating biological characteristics of marine renewable energy sites for environmental monitoring. M.Sc. thesis. Univ. of Washington.
- Williamson, B. J., B. E. Scott, J. J. Waggitt, C. Hall, E. Armstrong, P. Blondel, and P. S. Bell. 2014. Field deployments of a self-contained subsea platform for acoustic monitoring of the environment around marine renewable energy structures. *In Proceedings of Oceans 2014 MTS/IEEE, St John's, Canada, 2014.* doi:10.1109/oceans.2014.7003143
- Williamson, B. J., P. Blondel, E. Armstrong, P. S. Bell, C. Hall, J. J. Waggitt, and B. E. Scott. 2015. A self-contained subsea platform for acoustic monitoring of the environment around marine renewable energy devices – field deployments at wave and tidal energy sites in Orkney, Scotland. *IEEE J. Oceanic Eng.* **41**: 67–81. doi:10.1109/joe.2015.2410851
- Williamson, B. J., S. Fraser, P. Blondel, P. S. Bell, J. J. Waggitt, and B. E. Scott. In press. Multi-sensor acoustic tracking of fish and seabird behavior around tidal turbine structures in Scotland, UK. *IEEE J. Oceanic Eng.*

Acknowledgments

This work is funded by the Environment and Food Security theme Ph.D. studentship from the University of Aberdeen, the Natural Environment Research Council (NERC) and Department for Environment, Food, and Rural Affairs (Defra grant NE/J004308/1), and the Marine Collaboration Research Forum (MarCRF). We would like to gratefully acknowledge the support from colleagues at Marine Scotland Science.

Conflict of Interest

None declared.

Submitted 14 April 2016
Revised 23 September 2016
Accepted 14 November 2016

Associate editor: Craig Lee